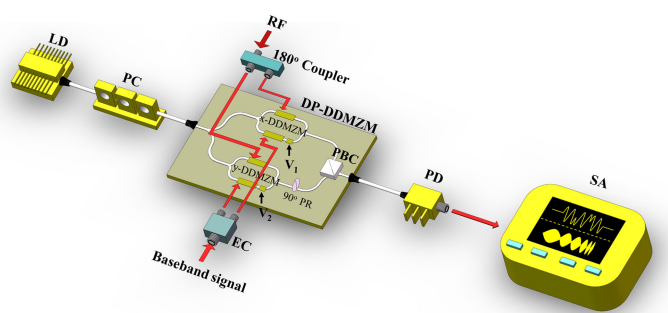# Photonic Scheme for the Generation of Background-Free Phase-Coded Microwave Pulses and Dual-Chirp Microwave Waveforms

Guangyi Li
Difei Shi
Zhiyao Jia
Lu Wang
Ming Li
Ning Hua Zhu
Wei Li

Photonic Scheme for the Generation of Background-Free Phase-Coded Microwave Pulses and Dual-Chirp Microwave Waveforms

Guangyi Li [ID],[1,2,3] **Difei Shi,**[1,2,3] **Zhiyao Jia** [ID],[1,2,3] **Lu Wang,**[1,2,3] **Ming Li** [ID],[1,2,3] **Ning Hua Zhu** [ID],[1,2,3] **and Wei Li** [ID][1,2,3]

[1]State Key Laboratory on Integrated Optoelectronics, Institute of Semiconductors, Chinese Academy of Sciences, Beijing 100083, China
[2]School of Electronic, Electrical and Communication Engineering, University of Chinese Academy of Sciences, Beijing 100049, China
[3]Center of Materials Science and Optoelectronics Engineering, University of Chinese Academy of Sciences, Beijing 100190, China

Abstract: We propose a photonic scheme to generate binary phase-coded microwave pulses and dual-chirp microwave waveforms without baseband-modulated signals (background noise) based on a dual-polarization dual-drive Mach-Zehnder modulator (DP-DDMZM) which contains x-DDMZM and y-DDMZM at two different polarization states. A radio frequency (RF) signal from a microwave source is transferred into two differential RF signals and employed into one arm of x-DDMZM and one arm of y-DDMZM, while a baseband signal from an arbitrary waveform generator is divided by an electronic coupler and then driven into the two other arms of DP-DDMZM. By adjusting the phase differences between the x-DDMZM and the y-DDMZM, binary phase-coded pulses and dual-chirp signals without baseband-modulated signals are generated. The proposed scheme can eliminate the interference caused by baseband-modulated signals, and satisfy different radar applications for different frequency bands. Experimental results show that phase-coded signals at 15 GHz with the bit rates of 1 Gb/s and 2 Gb/s and dual-chirp signals at 10 GHz and 15 GHz with the time durations of 0.5 μs are successfully generated. The reported scheme is well analyzed in theory and verified by experiment.

Index Terms: Microwave photonics, microwave generation, phase-coded signal, dual-chirp.

1. Introduction

Pulse compression has been extensively applied to realize both large detection range and high range resolution simultaneously in modern radar system. In order to obtain large pulse compression factor, spread spectrum microwave waveforms with large time bandwidth product are required [1], [2]. Phase-coded microwave waveforms and linearly chirped microwave waveforms

are two commonly utilized types of spread spectrum microwave waveforms in real-word application. Traditionally, a phase-coded or chirped microwave waveform is obtained through electronic circuits. However, it is difficult for electronic devices to generate microwave waveforms with high central frequency and large bandwidth. Compared with traditional electrical methods of generating phase-coded or chirped microwave waveforms, photonic generation has inherent advantages, such as light weight, large bandwidth, flexible tunability and immunity to electromagnetic interference. Therefore, photonic techniques for the generation of microwave waveforms have been widely studied to overcome the limitations of bottleneck in electrical domain [3], [4].

Numerous photonic methods for the generation of phased-coded microwave waveforms have been proposed [5]–[13]. In [5], [6], phase-coded signals or chirped signals with large bandwidth are generated by space-to-time mapping. In this technique, the system is bulky, lossy and has poor stability since spatial light modulator is used. Moreover, phase-coded signals can be generated by the spectral shaping followed by a dispersion element to perform frequency-to-time mapping [7], [8]. The technique can be utilized to generate arbitrary waveforms. Whereas, the reconfiguration of the waveform is not flexible since the tuning of the spectral response of the optical filter or the dispersion element is not easy. Phase-coded signals can also be realized by external modulation and optical heterodyning [9], [10]. In [9], phase-coded signal is generated by a Mach-Zehnder modulator (MZM) incorporated with a fiber Bragg grating (FBG) and a phase modulator (PM). However, the system is highly sensitive to the wavelength of optical carrier since a FBG is utilized. In [10], continuous-wave phase-coded signal is generated by a dual-parallel Mach-Zehnder modulator (DPMZM). Whereas, a baseband signal exists and it is noted that baseband-modulated signal (background noise) brings interference into different frequency bands, the performance of system would be degraded. Thus, some photonic methods of generating background-free phase-coded microwave waveforms are studied. In [11], phase-coded signals centered at different frequencies are generated by setting modulation indices at 3.83 rad and 5.13 rad. However, power fluctuation would deteriorate the performance of the system since the proposed system is sensitive to the power of the applied RF signal. In [12] and [13], the background-free phase-coded microwave waveforms are generated based on a dual-polarization dual-parallel Mach-Zehnder modulator (DP-DPMZM). In these methods, optical signals at orthogonal polarizations after the DP-DPMZM should be precisely adjusted by a polarization controller (PC), which increases the complexity of the system.

For linearly chirped microwave waveform, the range-Doppler resolution is degraded due of its knife-edge-type ambiguity function. In addition, this kind of ambiguity function brings large range-Doppler coupling, which decreases the measurement accuracy for moving targets [2], [14]. Hence, dual-chirp microwave waveform is introduced to address this issue. The dual-chirp microwave waveform is composed of two complementarily chirped signals within the same period. By analyzing the arrival times of up-chirped and down-chirped signals, the deterioration caused by range-Doppler coupling can be cancelled out. So far, a number of photonic methods of generating dual-chirp microwave waveforms have been reported. In [15]–[19], the dual-chirp microwave waveforms are obtained based on a DPMZM [15], two cascaded MZMs [16], a DP-DPMZM [17], a Fourier domain mode-locked optoelectronic oscillator [18], and an optically injected semiconductor laser [19]. However, the above-mentioned approaches are only utilized to generate microwave waveforms in a single format. Multi-format signals are highly desirable for multi-functional radar applications to fulfill different needs, such as anti-interception ability and high resolution. Photonic approaches for generating multi-format signals are studied in [20], [21]. In [20], a photonic method for the generation of switchable chirped signals based on DPMZM is proposed. By adjusting the bias voltage of the DPMZM, dual-, up-, and down-chirp waveforms can be generated successfully. The proposed approach has a compact structure which is promising for radar applications. Also, in [21], a photonic method for the generation of both chirped signals and phase-coded signals are proposed. By adjusting bias voltages and the power of the input microwave signals, chirped and phase-coded microwave waveforms can be generated after photodetection. However, the generated background noise decreases the power efficiency, which needs to be removed using electrical filters in practice.
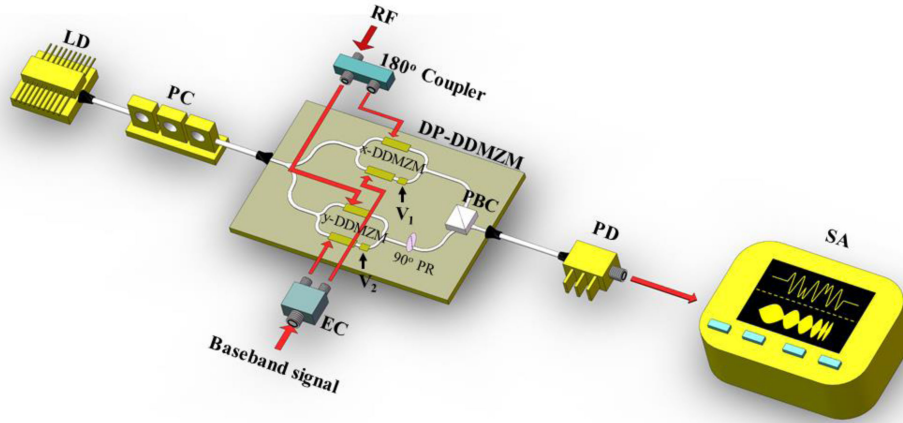
Fig. 1. Schematic diagram of the proposed multi-format microwave signals generator. LD: laser diode; PC: polarization controller; DP-DDMZM: dual-polarization dual-drive Mach-Zehnder modulator; 90° PR: 90° polarization rotator; PBC: polarization beam combiner; PD: photodetector; SA: signal analyzer; RF: radio frequency; EC: electrical coupler.

In this paper, we propose and demonstrate a photonics-based microwave signal generator which can generate phase-coded and dual-chirp signals without baseband-modulated signals. The main component is a dual-polarization dual-drive Mach-Zehnder modulator (DP-DDMZM) which includes two DDMZMs at two polarization states (x-DDMZM and y-DDMZM). The RF signal from a microwave source is transferred into two differential signals. The baseband signal from an arbitrary waveform generator (AWG) is divided into two same baseband signals by an electrical coupler. The differential RF signals and the two same baseband signals are driven into the four arms of DP-DDMZM. The phase differences of x-DDMZM and y-DDMZM are set at 0 and π, respectively. The background-free phase-coded microwave pulses at 15 GHz with the bit rates of 1 Gb/s and 2 Gb/s and dual-chirp microwave waveforms at 10 GHz and 15 GHz with the time durations of 0.5 μs are successfully generated. The generated microwave waveforms exclude baseband-modulated terms, which is preferred for radar applications at different frequency bands. In addition, the whole system has a compact and simple structure, which reduces the complexity of the system and improves the performance for real-world applications.

2. Principle

The schematic configuration of the proposed method of generating phase-coded and dual-chirp microwave waveforms is displayed in Fig. 1. The linearly polarized incident light from a laser diode (LD) is coupled into a DP-DDMZM through a PC. The DP-DDMZM which consists of two sub-DDMZMs (x-DDMZM and y-DDMZM) and a 90° polarization rotator is utilized to generate two orthogonally polarized optical signals. An RF signal $V\cos(2\pi ft)$ from an external microwave source is transferred into two differential RF signals, namely RF1 $= (V/2)\cos(2\pi ft)$ and RF2 $= -(V/2)\cos(2\pi ft)$. V and f are the original amplitude and frequency of the RF signal, respectively. The transferred signals are employed to one arm of x-DDMZM and one arm of y-DDMZM. A baseband signal $V_s s(t)$ from an AWG is divided into two same baseband signals by an electrical coupler and then applied to two other arms of DP-DDMZM. V_s is the amplitude of the original electrical baseband signal. The phase differences of the upper and lower DDMZMs introduced by voltage biases V_1 and V_2 are adjusted at $\alpha_1 = \pi(V_1)/V_\pi$ and $\alpha_2 = \pi(V_2)/V_\pi$, respectively. V_π is the half voltage of DP-DDMZM. At the output of DP-DDMZM, the optical filed can be mathematically expressed as

$$E = \begin{bmatrix} E_x(t) \\ E_y(t) \end{bmatrix} = \frac{\sqrt{2}}{4} E_\omega e^{j2\pi f_\omega t} \begin{bmatrix} e^{j\beta_c \cos(2\pi ft)} + e^{j\beta_s s(t) + j\alpha_1} \\ e^{-j\beta_c \cos(2\pi ft)} + e^{j\beta_s s(t) + j\alpha_2} \end{bmatrix}, \tag{1}$$

where E_ω and f_ω are the amplitude and the frequency of the optical carrier; $\beta_c = \pi(V/2)/V_\pi$ and $\beta_s = \pi(V_s/2)/V_\pi$ are the modulation indices for the differential RF signals and baseband signals, respectively.

After photodetection, the photocurrent is given by

$$
\begin{aligned}
i(t) &\propto E(t) \cdot E(t)^* \\
&\propto E_x(t) \cdot E_x(t)^* + E_y(t) \cdot E_y(t)^* \\
&\propto DC + |E_\omega|^2 \left\{ \cos[\beta_s s(t) + \alpha_1 - \beta_c \cos(2\pi f t)] + \cos[\beta_s s(t) + \alpha_2 + \beta_c \cos(2\pi f t)] \right\} \\
&= DC + |E_\omega|^2 \{ \cos[\beta_s s(t) + \alpha_1] \cos[\beta_c \cos(2\pi f t)] + \sin[\beta_s s(t) + \alpha_1] \sin[\beta_c \cos(2\pi f t)] \\
&\quad + \cos[\beta_s s(t) + \alpha_2] \cos[\beta_c \cos(2\pi f t)] - \sin[\beta_s s(t) + \alpha_2] \sin[\beta_c \cos(2\pi f t)] \} \\
&= DC + |E_\omega|^2 \cos[\beta_c \cos(2\pi f t)] \{ \cos[\beta_s s(t)][\cos(\alpha_1) + \cos(\alpha_2)] - \sin[\beta_s s(t)][\sin(\alpha_2) + \sin(\alpha_1)] \} \\
&\quad + |E_\omega|^2 \sin[\beta_c \cos(2\pi f t)] \{ \cos[\beta_s s(t)][\sin(\alpha_1) - \sin(\alpha_2)] + \sin[\beta_s s(t)][\cos(\alpha_1) - \cos(\alpha_2)] \}, \quad (2)
\end{aligned}
$$

where DC represents the direct current term. Under the condition that the α_1 and α_2 are defined as $\alpha_2 = \alpha_1 + \pi$ and Jacobi-Anger expansion is applied, Eq. (2) can be rewritten as

$$
\begin{aligned}
i(t) &\propto DC + |E_\omega|^2 \left\{ -2 \sum_{n=1}^{\infty} (-1)^n J_{2n-1}(\beta_c) \cos[(2n-1)(2\pi f t)] \right\} \\
&\quad \times \{ \cos[\beta_s s(t)][\sin(\alpha_2) - \sin(\alpha_1)] + \sin[\beta_s s(t)][\cos(\alpha_1) - \cos(\alpha_2)] \}, \quad (3)
\end{aligned}
$$

where J_n is the nth-order Bessel function of the first kind. Under small-signal modulation, only first order term is considered. If α_1 and α_2 are chosen to be 0 and π, Eq. (3) can be expressed as

$$
i(t) \propto DC + 4|E_\omega|^2 J_1(\beta_c) \cos(2\pi f t) \sin[\beta_s s(t)]. \quad (4)
$$

Firstly, $s(t)$ is set to be a three-level electrical coding signal, namely $s(t) = \{0, -1, +1\}$. It is noted that if $s(t)$ equals 0, no microwave signal is generated after the photodetection. If the value of $s(t)$ changes between +1 and -1, the precise π phase shift is introduced. Therefore, a background-free phase-coded microwave waveform is generated. Moreover, it should be noted that the phase shift is dependent on the polarity of the electrical coding signal instead of its amplitude, which is easier to implement and decreases the power consumption of the whole system.

Secondly, if $s(t)$ is a single-chirp signal, namely $s(t) = \cos(kt^2)$. Using Jacobi-Anger expansion and small-signal modulation, Eq. (4) can be rewritten as

$$
\begin{aligned}
i(t) &\propto DC + 4|E_\omega|^2 J_1(\beta_c) \cos(2\pi f t) \sin[\beta_s \cos(kt^2)] \\
&\propto DC + 8|E_\omega|^2 J_1(\beta_c) \cos(2\pi f t) J_1(\beta_s) \cos(kt^2) \\
&= DC + 4|E_\omega|^2 J_1(\beta_c) J_1(\beta_s)[\cos(2\pi f t + kt^2) + \cos(2\pi f t - kt^2)]. \quad (5)
\end{aligned}
$$

It can be seen that a dual-chirp microwave waveform without baseband-modulated term is realized. Consequently, multi-format background-free microwave waveforms are generated.

3. Experimental Results and Discussion

A proof-of-concept experiment based on the configuration shown in Fig. 1 was implemented to demonstrate the proposed multi-format microwave waveforms generator. Firstly, the generation of background-free phase-coded pulses was experimentally verified. The wavelength and optical power of the continuous-wave light emitted from a laser diode were 1550.150 nm and 10 dBm. The linearly polarized optical signal was coupled into a DP-DDMZM (Fujitsu, FTM7980EDA). The two differential RF signals were driven into one arm of x-DDMZM and one arm of y-DDMZM. The baseband signal was a three-level electrical coding signal from an AWG. The baseband signal was divided by an electrical coupler and fed into the two other arms of DP-DDMZM. In addition, the
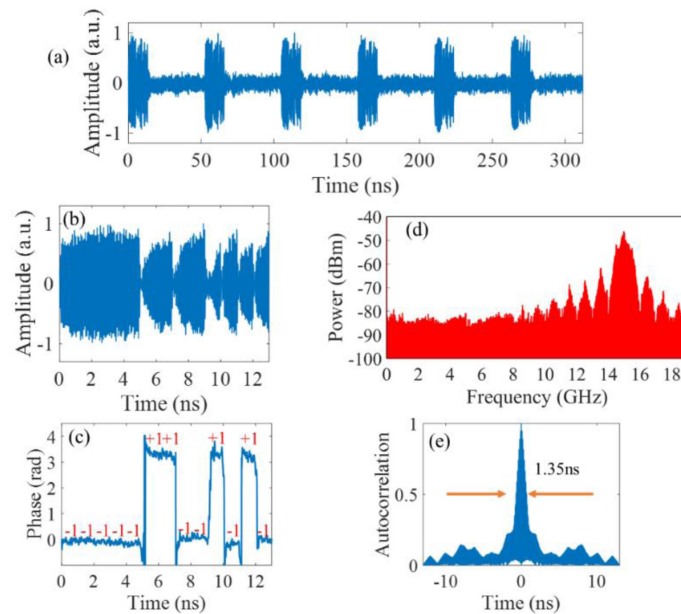
Fig. 2. (a) Waveform in 312 ns, (b) waveform in 13 ns, (c) phase information extracted from (b) using Hilbert transform, (d) electrical spectrum and (e) autocorrelation of phase-coded microwave signal centered at 15 GHz with a bit rate of 1 Gb/s.

phase difference of x-DDMZM and y-DDMZM were set at 0 and π as described in the theoretical part. The optical signals at the two orthogonal polarization states from the output of the DP-DDMZM were sent into a PD with a 3-dB bandwidth of 18 GHz. After photodetection, the background-free phase-coded pulses were successfully generated. The electrical spectrum and the waveform were monitored by an electrical spectrum analyzer and an electrical oscilloscope, respectively.

The coding signal was defined as a 52-bit fixed pattern, which was a series of 13-bit Baker code pulses (-1, -1, -1, -1, -1, +1, +1, -1, -1, +1, -1, +1, -1) followed by 39-bit 0 with a peak-to-peak amplitude of 0.1 V. Fig. 2 illustrates the experimental results of a background-free phase-coded microwave pulse with a bit rate of 1 Gb/s. Fig. 2(a) displays the waveforms in 312 ns, which are in pulse mode. The DC term has no effect on the shape of the wanted binary phase-coded microwave pulse, so the DC term is aligned at 0 in order to realize the normalization of waveform. Fig. 2(b) exhibits the waveform in 13 ns and the obvious phase shifts can be seen. Hilbert transform was utilized to extract the phase information of the generated phase-coded signal, and the extracted phase shift information shown in Fig. 2(c) matches well with the electrical Baker coding signal. Fig. 2(d) is the electrical spectrum of the phase-coded signal, and it can also be seen that no baseband-modulated term is generated. In addition, the autocorrelation of the generated phase-coded microwave waveform was calculated to evaluate the performance of pulse compression as displayed in Fig. 2(e). The full width at half-maximum (FWHM) is 1.35 ns, the pulse compression ratio (PCR) is 9.63.

To show that our generator has wider application, the background-free phase-coded pulses centered at 15 GHz with a bit rate of 2 Gb/s have been generated and the experimental results are illustrated in Fig. 3. Fig. 3(a) shows the microwave pulses in 156 ns. Fig. 3(b) shows the waveform in 6.5 ns, and Fig. 3(c) is the phase shift information extracted from Fig. 3(b) using Hilbert transform. It can be seen that the extracted phase information fits well with the electrical Baker coding signal. Fig. 3(d) exhibits the electrical spectrum, which verifies that the experimental results exclude baseband-modulated term. Fig. 3(e) is the autocorrelation result of the generated signal. The FWHM and PCR are 0.61 ns and 10.66, respectively.

As for the generation of dual-chirp microwave waveforms, the baseband signal was chosen to be a single-chirp with a bandwidth of 0.5 GHz and a time duration of 0.5 μs. Similarly, the single-chirp
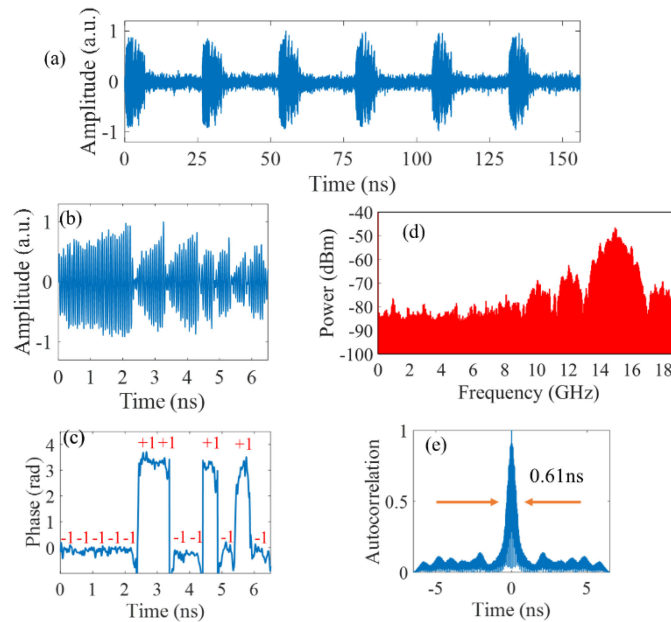
Fig. 3. (a) Waveform in 156 ns, (b) waveform in 6.5 ns, (c) phase information extracted from (b) using Hilbert transform, (d) electrical spectrum and (e) autocorrelation of phase-coded microwave signal centered at 15 GHz with a bit rate of 2 Gb/s.

baseband signal was divided by an electrical power coupler and then employed into two arms of DP-DDMZM as described in theoretical part. The two other arms of the DDMZM were fed by two differential RF signals. By adjusting the direct current voltages, two DDMZMs were biased at the maximum transmission point and minimum transmission point, respectively. The x-polarized and y-polarized optical signals from the DP-DDMZM were sent into the PD. Afterwards, the dual-chirp microwave waveforms centered at high frequency band were obtained.

In order to show the tunability of our proposed configuration, two RF signals at 10 GHz and 15 GHz were selected to carry out the experiment. The experimental results of dual-chirp microwave waveforms are illustrated in Fig. 4. Fig. 4(a) and Fig. 4(e) show the temporal waveforms of dual-chirp signals centered at 10 GHz at 15 GHz with the time durations of 0.5 μs. Fig. 4(b) displays the instantaneous frequency-time diagram of the generated dual-chirp microwave waveform using short time Fourier transform. Obviously, a dual-chirp waveform with an up-chirp from 10 GHz to 10.5 GHz and a down-chirp from 10 GHz to 9.5 GHz was successfully generated. Similarly, Fig. 4(f) shows the instantaneous frequency-time diagram of dual-chirp signal consisting of an up-chirp from 15 GHz to 15.5 GHz and a down-chirp from 15 GHz to 14.5 GHz. Fig. 4(c) and Fig. 4(g) exhibit the electrical spectra of the generated dual-chirp waveforms, which demonstrates that the baseband-modulated signals are cancelled out. In addition, the corresponding autocorrelations of dual-chirp microwave waveforms were calculated to show the performance of pulse compression. Fig. 4(d) shows the autocorrelation of the dual-chirp centered at 10 GHz, and the FWHM and PCR are 1.40 ns and 357, respectively. The autocorrelation of the generated dual-chirp centered at 15 GHz is shown in Fig. 4(h). The FWHM and PCR are 1.41 ns and 355. As can be seen, the pulse compression of the generated dual-chirp signals has a good performance. Furthermore, the central frequency of dual-chirp microwave can be increased if a PD with large bandwidth is used in our experiment. The proposed scheme can fulfill the needs for radar applications working at different frequency bands. Moreover, since all the components utilized in the proposed approach can be covered by current hybrid photonic integration technologies [22]. A photonic integrated circuit replica of the system is a promising solution to further reduce the size, power consumption and cost.
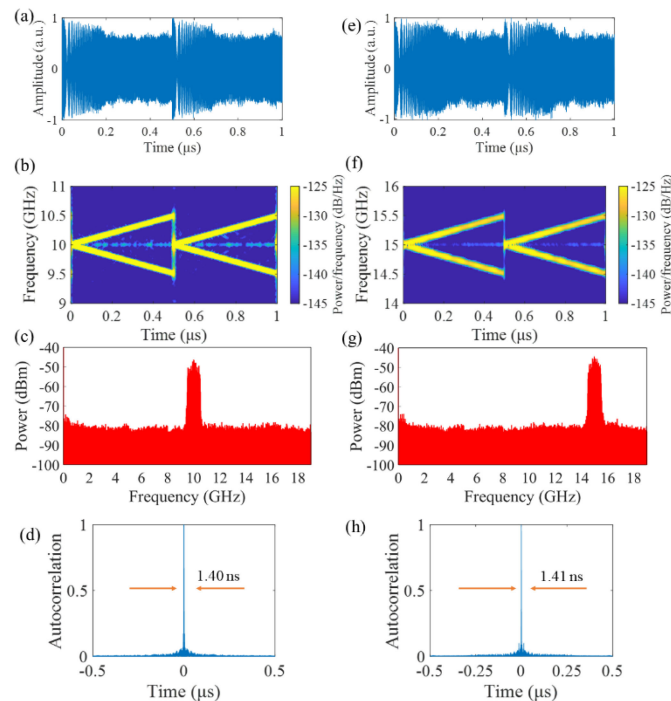
Fig. 4. (a) and (e) Waveforms, (b) and (f) frequency-time diagrams, (c) and (g) electrical spectra, and (d) and (h) autocorrelation of generated dual-chirp signals centered at 10 GHz and 15 GHz.

4. Conclusion

In conclusion, we have analyzed and demonstrated a photonic configuration to generate background-free phase-coded microwave pulses and dual-chirp microwave waveforms. The DP-DDMZM used in the configuration is fed by two differential RF signals and two same baseband signals, and the two DDMZMs at two polarization states are biased at maximum transmission point and minimum transmission point, respectively. Background-free phase-coded microwave pulses centered at 15 GHz with the bit rates of 1 Gb/s and 2 Gb/s are successfully generated. The precise π phase shift depends only on the polarity of the applied coding signal rather than its amplitude, which decreases the power consumption. In addition, dual-chirp microwave waveforms centered at 10 GHz and 15 GHz are also successfully realized. A compact and stable structure is realized since only one modulator is involved. The elimination of baseband-modulated signals increases the performance of the proposed scheme in radar system and makes it more suitable for radar antennas which work at different frequency bands. Therefore, our proposed scheme might offer promising applications for modern radar and electronic warfare systems.

References

[1] M. I. Skolnik, *Introduction to Radar Systems*. 3rd ed., New York, NY, USA: McGraw-Hill, 2001.
[2] M. A. Richards, *Fundamentals of Radar Signal Processing*. 2nd ed., New York, NY, USA: McGraw-Hill, 2014.
[3] J. Yao, "Microwave photonics," *J. Lightw. Technol.*, vol. 27, no. 3, pp. 314–335, Feb. 2009.
[4] J. Capmany, and D. Novak, "Microwave photonics combines two worlds," *Nat. Photon.*, vol. 1, no. 6, pp. 319–330, Jun. 2007.
[5] J. D. McKinney, D. E. Leaird, and A. M. Weiner, "Millimeter-wave arbitrary waveform generation with a direct space-to-time pulse shaper," *Opt. Lett.*, vol. 27, no. 15, pp. 1345–1347, Aug. 2002.
[6] M. Shen, and R. A. Minasian, "Toward a high-speed arbitrary waveform generation by a novel photonic processing structure," *IEEE Photon. Technol. Lett.*, vol. 16, no. 4, pp. 1155–1157, Apr. 2004.
[7] J. Ye *et al.*, "Photonic generation of microwave phase-coded signals based on frequency-to-time conversion," *IEEE Photon. Technol. Lett.*, vol. 24, no. 17, pp. 1527–1529, Sep. 2012.

[8] F. Zhang, X. Ge, S. Pan, and J. Yao, "Photonic generation of pulsed microwave signals with tunable frequency and phase based on spectral-shaping and frequency-to-time mapping," *Opt. Lett.*, vol. 38, no. 20, pp. 4256–4259, Oct. 2013.

[9] H. Y. Jiang, L. S. Yan, J. Ye, W. Pan, B. Luo, and X. Zou, "Photonic generation of phase-coded microwave signals with tunable carrier frequency," *Opt. Lett.*, vol. 38, no. 8, pp. 1361–1363, Apr. 2013.

[10] Y. Yu, J. Dong, F. Jiang, and X. Zhang, "Photonic generation of precisely π phase-coded microwave signal with broadband tunability," *IEEE Photon. Technol. Lett.*, vol. 25, no. 24, pp. 2466–2469, Dec. 2013.

[11] Y. Chen, and S. Pan, "Photonic generation of tunable frequency-multiplied phase-coded microwave waveforms," *IEEE Photon. Technol. Lett.*, vol. 30, no. 13, pp. 1230–1233, Jul. 2018.

[12] S. Zhu, M. Li, X. Wang, N. H. Zhu, Z. Z. Cao, and W. Li, "Photonic generation of background-free binary phase-coded microwave pulses," *Opt. Lett.*, vol. 44, no. 1, pp. 94–97, Jan. 2019.

[13] X. Li, S. Zhao, S. Pan, Z. Zhu, K. Qu, and T. Lin, "Generation of a frequency-quadrupled phase-coded signal using optical carrier phase shifting and balanced detection," *Appl. Opt.*, vol. 56, no. 4, pp. 1151–1156, Feb. 2017.

[14] R. J. Fitzgerald, "Effects of range-Doppler coupling on chirp radar tracking accuracy," *IEEE Trans. Aerosp. Electron. Syst.*, vol. AES-10, no. 4, pp. 528–532, Jul. 1974.

[15] D. Zhu, and J. Yao, "Dual-chirp microwave waveform generation using a dual-parallel Mach-Zehnder modulator," *IEEE Photon. Technol. Lett.*, vol. 27, no. 13, pp. 1410–1413, Jul. 2015.

[16] Y. Xu, T. Jin, H. Chi, S. Zheng, X. Jin, and X. Zhang, "Photonic generation of dual-chirp waveforms with improved time-bandwidth product," *IEEE Photon. Technol. Lett.*, vol. 29, no. 15, pp. 1253–1256, Aug. 2017.

[17] X. Li, S. Zhao, Z. Zhu, K. Qu, T. Lin, and D. Hu, "Photonic generation of frequency and bandwidth multiplying dual-chirp microwave waveform," *IEEE Photon. J.*, vol. 9, no. 3, Jun. 2017, Art. no. 7104014.

[18] T. Hao, J. Tang, N. Shi, W. Li, N. Zhu, and M. Li, "Dual-chirp Fourier domain mode-locked optoelectronic oscillator," *Opt. Lett.*, vol. 44, no. 8, pp. 1912–1915, Apr. 2019.

[19] P. Zhou, H. Chen, N. Li, R. Zhang, and S. Pan, "Photonic generation of tunable dual-chirp microwave waveforms using a dual-beam optically injected semiconductor laser," *Opt. Lett.*, vol. 45, no. 6, pp. 1342–1345, Mar. 2020.

[20] C. Yi, S. Yang, B. Yang, T. Jin, and H. Chi, "Photonic approach for generating bandwidth-doubled and switchable multi-format chirp waveforms," *Opt. Lett.*, vol. 46, no. 7, pp. 1578–1581, Apr. 2021.

[21] L. Wang *et al.*, "Photonic generation of multiband and multi-format microwave signals based on a single modulator," *Opt. Lett.*, vol. 45, no. 22, pp. 6190–6193, Oct. 2020.

[22] D. Marpaung, J. Yao, and J. Capmany, "Integrated microwave photonics," *Nature Photon.*, vol. 13, no. 2, pp. 80–90, Jan. 2019.